Bi-directional Battery Charging/Discharging Converter for Grid Integration: A Step Towards Power Quality and Efficient Energy Management in Electric Vehicles

Anas Diouri[1,*], *Mohamed* Khafallah[1], *Abdelilah* Hassoune[1] and *Mohammed Amine* Meskini[1]

[1]Laboratory of Energy & Electrical Systems (LESE), Superior National School of Electricity and Mechanical (ENSEM), Hassan II University of Casablanca, 20470 Casablanca, Morocco

Abstract. This paper presents the design and simulation of a bi-directional battery charging and discharging converter capable of interacting with the grid. The proposed converter enables Electric Vehicles (EVs) not only to charge their batteries from the grid but also to discharge excess energy back into the grid through the Vehicle-to-Grid (V2G) operating mode. The work discusses charger design considerations, including control strategies, and examines its potential contribution to efficient energy management and grid stability. Furthermore, a simulation study using MATLAB/Simulink validates the performance, efficiency, and dynamic response of the bi-directional converter, demonstrating its viability for real-world grid integration. The simulation shows better performance in various performance aspects, including high-power factor correction (PFC), minimized steady-state oscillations, reduced DC link voltage overshoot, increased overall efficiency, and both voltage and current Total Harmonic Distortions (THD maintained below 5%).

1 Introduction

The awareness of the significant impact of carbon dioxide emissions from traditional Internal Combustion Engine (ICE) vehicles has underscored the pressing need to enhance the electrification of the transportation sector. This urgency arises from the realization that merely charging Electric Vehicles (EVs) from conventional fossil fuel-based sources doesn't effectively reduce carbon emissions. Instead, it shifts the emissions from the EVs to the power plants supplying the energy. With the number of EVs growing at an unprecedented rate, there's a substantial surge in electric demand. This makes the present moment crucial for both EV owners and electric utilities to explore innovative methods of charging EVs using reliable and environmentally-friendly energy sources, with the aim of minimizing emissions and optimizing charging costs [1,2].

In recent times, there has been a notable surge in interest towards bidirectional power flow between the grid and EV batteries. Bidirectional converters stand as the fundamental technology, empowering vehicles to transform into dynamic mobile energy storage systems. With chargers capable of seamless power transfer in both directions, EVs transcend their conventional role as mere vehicles, evolving into integral battery storage units for intermittent energy sources. This groundbreaking capability enables EV batteries to be charged and subsequently discharge stored energy back to the grid through the same connection. Realizing this bidirectional power integration demands sophisticated and intelligent converters endowed with advanced control systems [4]. This marks a pivotal shift towards the effective utilization of EVs as distributed battery energy storage systems. However, achieving this transformative integration requires a meticulous consideration of several crucial factors, including size, weight, power density, reliability, efficiency, cost, and the control mechanism of these converters [5].

* Corresponding author: anas.diouri-etu@etu.univh2c.ma

According to multiple researchers, traditional converter topologies for EV chargers typically consist of a single-stage front-end AC-DC converter. In contrast, DC fast charging integrates a back-end DC-DC converter to enhance voltage regulation [3]. Meanwhile, bidirectional EV chargers take a step further, employing two stages of power conversion. This design allows for seamless connection of vehicles with varying voltage requirements through a single connector. In the initial stage, it operates as a rectifier during battery charging, seamlessly transitioning to an inverter when transferring power from the battery pack to the AC mains. The subsequent stage, managed by the DC-DC converter, steps down the voltage levels for efficient EV battery charging and amplifies voltage for smooth power transfer to the grid.

With the rapid progress in semiconductor technologies, bidirectional converters have become a focus of extensive research. These converters generally come in two main topologies: full-bridge and half-bridge. Half-bridge converters exhibit a few switching components, resulting in lower cost and excellent performance. However, they place higher stress on the elements. On the other hand, full-bridge converters experience an increase in cost as the number of components rises, but they mitigate stress on the devices [6].

This article presents a review of the leading converter technologies and topologies employed in V2G applications [7-9]. By examining these converter technologies, we can gain valuable insights into their strengths and limitations, ultimately contributing to the advancement and optimization of V2G technology. In Section 2, a comprehensive description is provided regarding the system configuration of the single-phase non-isolated bidirectional EV charger, along with an in-depth exploration of the passive components design within the charger. Section 3 elaborates the proposed charger controller for both converter stages: the bi-directional AC-DC and the bi-directional DC-DC converters. Furthermore, MATLAB/Simulink model and the simulation results of the proposed charger controller in both modes, charging and discharging are presented in Section 4. Finally, the key takeaways and conclusions are drawn in Section 5.

2 System description of the single phase non-isolated bidirectional EV charger

As the interface between an electric vehicle and a utility grid, the bidirectional converter is required to meet essential criteria from both the vehicle and grid. Fig.1 illustrates all the stages used to convert power from the grid to the EVs and back.

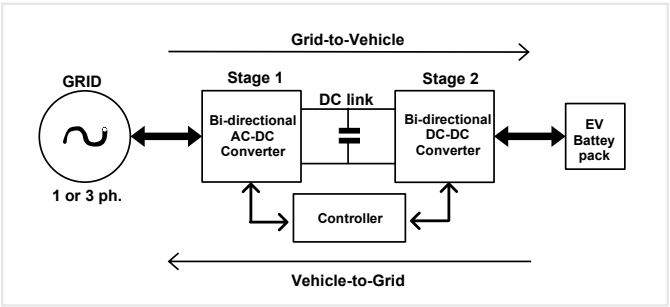

Fig. 1. Bi-directional EV Battery Charging/Discharging structure

The converter is a combination of a bidirectional AC-DC and a bidirectional DC-DC converter as shown in Fig2 [7]. First the bidirectional AC-DC converter operates in two modes, namely as front-end rectifier when power transfer is from the single-phase grid to the EV battery, and it works as a voltage source inverter while the EV battery is pushing back power to the source [10].

Then, the bidirectional buck-boost DC-DC converter operated as a back-end converter is intended for efficient electrical power transfer and battery charging [11]. During charging mode, the charger acts as a buck converter and as a boost converter while discharging.

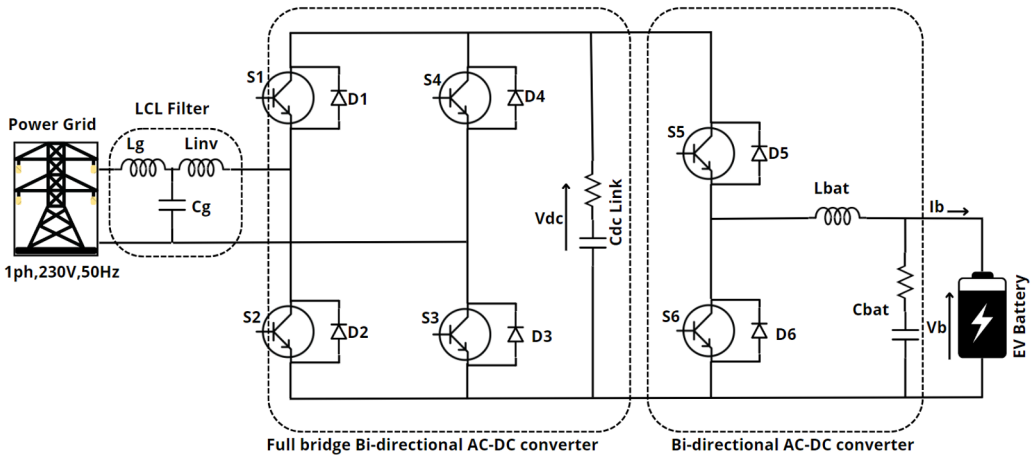

Fig. 2. Topology of the proposed Bi-directional EV Battery Charging/Discharging Circuit

2.1 LCL Filter design

The LCL filter serves a crucial role in refining the inverter current output, delivering a filtered current devoid of harmonics to the grid. The benefits of using LCL filters encompass substantial attenuation of unwanted frequencies, leading to enhanced overall performance, cost efficiency, and reduced weight and size. Importantly, the LCL filter achieves effective harmonic elimination even when utilizing relatively small inductor and capacitor values. Compared to other filter types, such as single-L or L-C filters, the LCL configuration offers distinct advantages. It provides superior attenuation of high-frequency harmonics, which is particularly beneficial in grid-tied applications where strict harmonic distortion limits must be met. Additionally, LCL filters demonstrate a wider bandwidth and better transient response, making them more adaptable to varying load conditions.

The inverter side inductance, Grid side inductance, and Grid side capacitance design are designed and calculated as follows [12,13]:

$$L_{inv} = \frac{V_{dc}}{4.f_{sw}.\Delta I_{max}} \tag{1}$$

$$L_g = \frac{10\%.V^2{}_g}{2.\pi.f_g.P} - L_{inv} \tag{2}$$

$$C_g = \frac{5\%.P}{2.\pi.f_g.V^2{}_g} \tag{3}$$

Where Vg, Vdc, $\Delta I max$, P, Fg and F_{sw} are the grid voltage, DC-link voltage, maximum inductor ripple current, rated power, grid frequency and switching frequency, respectively.

2.2 DC-link capacitance design

The DC link capacitor is the main energy-storing element; its sizing should be optimum so it can meet the specifications of the system. The determination of the DC link capacitance value is influenced by various factors such as the current ripple and the tolerable voltage ripple. The capacitor value of the DC link is defined as follows [14]:

$$C_{dc} = \frac{P}{2.\pi.f_g.V_{dc}.\Delta V} \tag{4}$$

2.3 Bi-directional Buck-Boost passive components design

The DC-DC converter role is to control charging and discharging operations of the battery according to the demanded power level. During charging mode, the DC link operates as an input for the bidirectional converter, and the EV battery is connected as the load on the output side. This configuration allows the converter to operate in a buck mode.

Conversely, in the discharging mode, the converter bridges the connection between the DC link and the battery. In this mode, the battery acts as the input source, while the DC link serves as the output [15,16].

2.3.1 Buck-Boost inductance design

The filter inductance at the battery side is designed and calculated as follows:

$$L_{buck} = \frac{(V_{dc} - V_b).D_{buck}}{f_{sw}.\Delta I} \ , (D_{buck} = \frac{V_b}{V_{dc}}) \tag{5}$$

$$L_{boost} = \frac{V_b.(V_{dc} - V_b)}{V_{dc}.f_{sw}.\Delta I} \tag{6}$$

$$L_{bat} = \max(L_{buck}, L_{boost}) \tag{7}$$

2.3.2 Buck-Boost capacitance design

The filter capacitance at the battery side is designed and calculated as follows:

$$C_{boost} = \frac{V_{dc}.D_{boost}}{R_0.\Delta V} \ , (D_{boost} = 1 - \frac{V_b}{V_{dc}}) \tag{8}$$

$$C_{buck} = \frac{\Delta I}{8.f_{sw}.\Delta V} \tag{9}$$

$$C_{bat} = \max(C_{buck}, C_{boost}) \tag{10}$$

3 The control system of the Battery Charging/Discharging Circuit

3.1 The proposed control diagram for stage 1

In Figure 3, the proposed control includes a voltage control loop. The voltage control loop samples dc link voltage, with respect to the predefined reference DC-link voltage ($V_{dc\text{-}ref}$), to produce the reference interfacing inductor current ($I_{nf\text{-}ref}$). In this process, a single-phase, phase-locked loop (PLL) is also incorporated to keep the input grid current sinusoidal and in phase with the grid voltage (Vg), to achieve the unity PF. Furthermore, the error obtained from the continuous comparison of ($I_{inv\ ref}$) and actual inverter current (I_N) is fed to a Proportional and Resonant Current controller (PR Controller) [17,18]. The PR Controller's output is then used to generate the necessary PWM signals for controlling the switching devices within the stage-1 converter. This systematic approach ensures efficient control and regulation of the entire system. Unlike conventional controllers, the PR Controller combines proportional control with resonance-based techniques, offering precise tracking of the grid current reference and robust damping of system resonances. This ensures enhanced stability and dynamic response, particularly in scenarios where grid conditions may vary. Furthermore, the PR Controller's inherent capability to address both transient and steady-state performance requirements made it the optimal choice for achieving efficient control and regulation within the entire system.

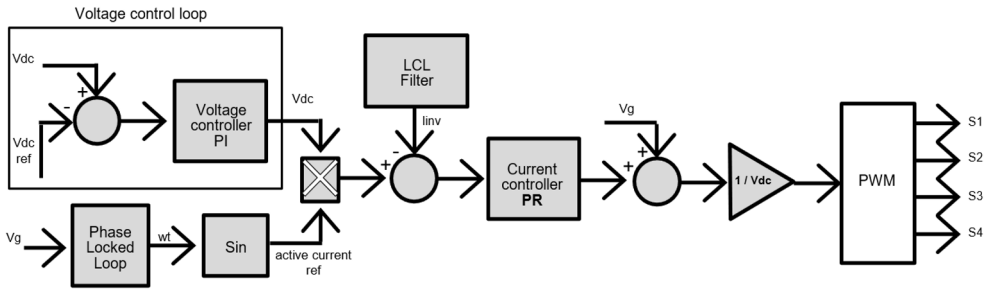

Fig. 3. Controller of bi-directional AC-DC converter (Stage1)

3.2 The proposed control diagram for bidirectional Buck-Boost converter

The control diagram is illustrated in Figure 4. In this process, the battery current (I_{bat}) and the reference current ($I_{bat\text{-}ref}$) are compared using a comparator. The resulting error signal is then fed into the current controller. The output of the current controller is determined by the difference between the current magnitude of the ongoing battery charging current (I_{bat}) and the reference ($I_{bat\text{-}ref}$) [19-21]. The PWM signal for the switches in the stage-2 converter, the duty cycle's adjustment is directly influenced by the output of the current controller.

Conversely, during boost mode, the current direction reverses, flowing from the battery. Despite this change, the rest of the configuration remains unaffected.

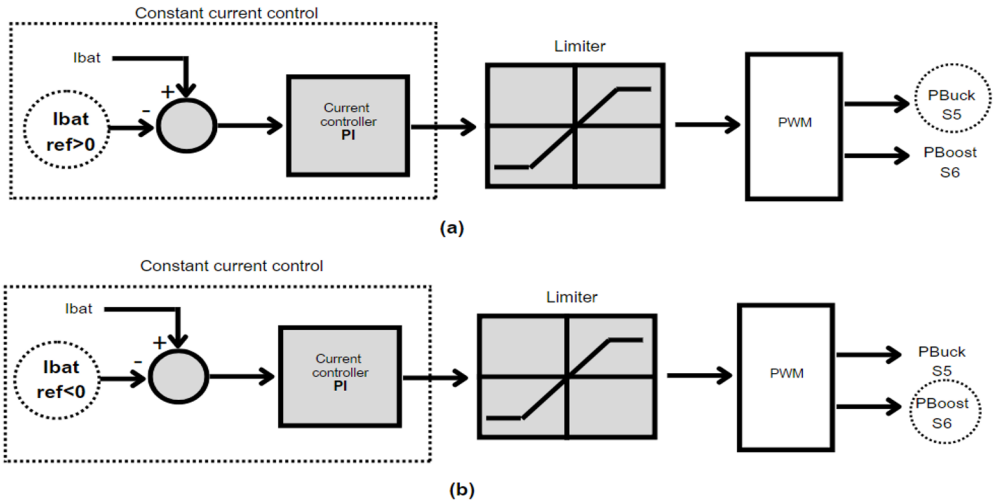

Fig. 4. Controller of bidirectional Buck-Boost converter (stage 2) : (a) Battery buck/charging mode control diagram ;

(b) Battery boost/discharging mode control diagram

4 Simulation results and discussion

The proposed single-phase non-isolated Bi-directional Battery Charging and Discharging Circuit is evaluated using MATLAB/Simulink to assess its performance. The schematic of the proposed charger, constructed using fundamental Simulink blocs is depicted in Fig. 5. The charger is assumed to have a rating of 2 kW, with a maximum charging current of 8.7 Amps at a charging voltage of 230 Volts. The chosen switching device for stage 1 is the IGBT from the Simscape library, featuring an internal resistance of 1 mΩ and a snubber resistance of 0.1 MΩ, and MOSFET as a switching device for stage 2, featuring an internal resistance of 10 mΩ and a snubber resistance of 0.1 MΩ. The system simulation employs a generic MATLAB battery model with a Lithium-ion battery type. The

simulation parameters for the proposed bi-directional charger are detailed in Table 3. For testing purposes, a battery nominal voltage of 160 V and a DC link voltage of 400 V are selected in this study. In addition, the design guideline and the system parameters used for simulation are presented in Table 1.

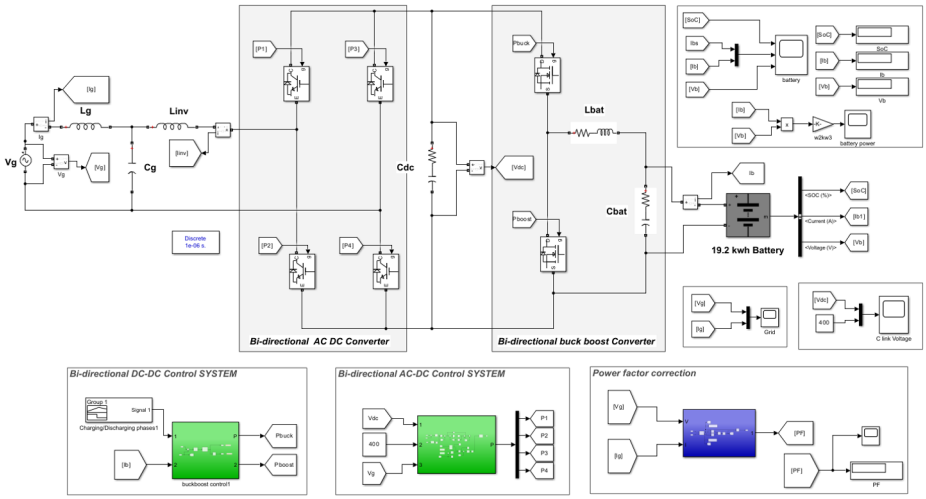

Fig. 5 Simulation model of the proposed Bi-directional Battery Charging/Discharging Circuit

Table 1. System parameters used for simulation

Notation	Parameter	Value
V_g	Grid voltage	230 V
f_g	Grid frequency	50 Hz
L_{inv}	Inverter side inductance	4.1 mH
L_g	Grid side inductance	4.4 mH
C_g	Grid side capacitance	6.25 uF
P	Charger rated power	2 KW
f_{sw}	Switching frequency for both converters	10 kHz
V_{dc}	DC-link voltage	400 V
C_{dc}	DC-link capacitance	5600 uF
L_{bat}	Battery side filter inductance	20 mH
C_{bat}	Battery side filter capacitance	100 uF
V_{bn}	Battery nominal voltage	160 V
Ah	Battery capacity	120 Ah
ΔI	Current ripple	20%
ΔV	Voltage ripple	5%
THD	Total harmonic distortion (THD)	<5%

Finally, the circuit has been simulated for a duration of 2 seconds, with the initial t = 1 second representing the discharging mode and the subsequent t = 1 second representing the charging mode. Moreover, comprehensive assessments of the performance in both modes are elaborated upon in the subsequent subsections.

4.1 Discharging operation (V2G Mode)

The discharging mode takes place from the EV battery to the grid, Fig. 6 confirms the unity power-factor operation during is this period and that the input grid current, is in phase with the input grid voltage Vg.

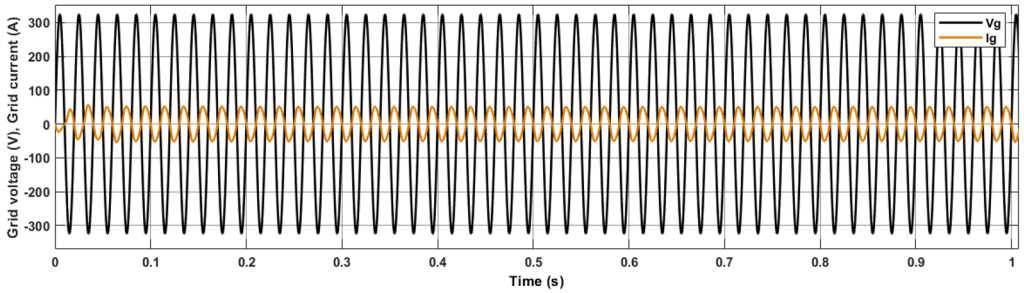

Fig. 6. Grid voltage and current during discharging mode (V2G)

Once the charger is connected to the grid, the voltage across the DC link capacitor gradually increases, as demonstrated in Fig. 7. The voltage attains its target level of 400V within an impressive timeframe of under 0.4 seconds, devoid of any noticeable overshoot. While some ripples are inevitable during steady-state operation due to converter switching, their magnitude is approximately 10V, which is acceptably low.

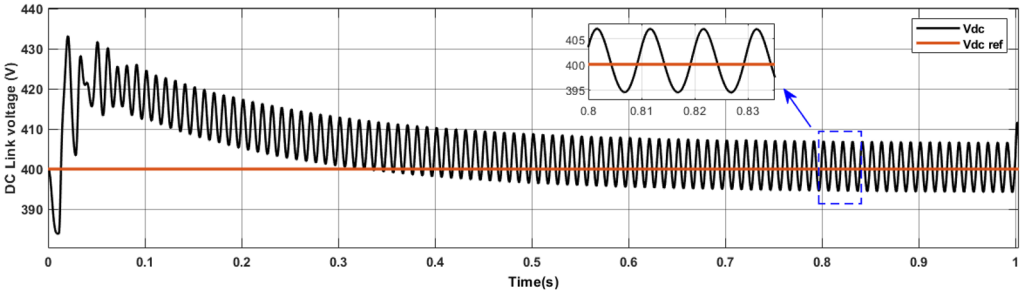

Fig. 7. DC-link voltage during discharging mode (V2G)

The EV battery performance is presented through the battery state of charge (SoC), charging current, and voltage, as exhibited in Fig. 8. Within the discharging mode segment, the reduction in SoC and the negative current value indicate the battery's discharge. Correspondingly, Fig. 9 visualizes the instantaneous energy or power stored in the EV batteries. Notably, negative power values indicate the battery discharging process. Furthermore, a unity PF is achieved using inverter control strategy, as shown in Fig. 10.

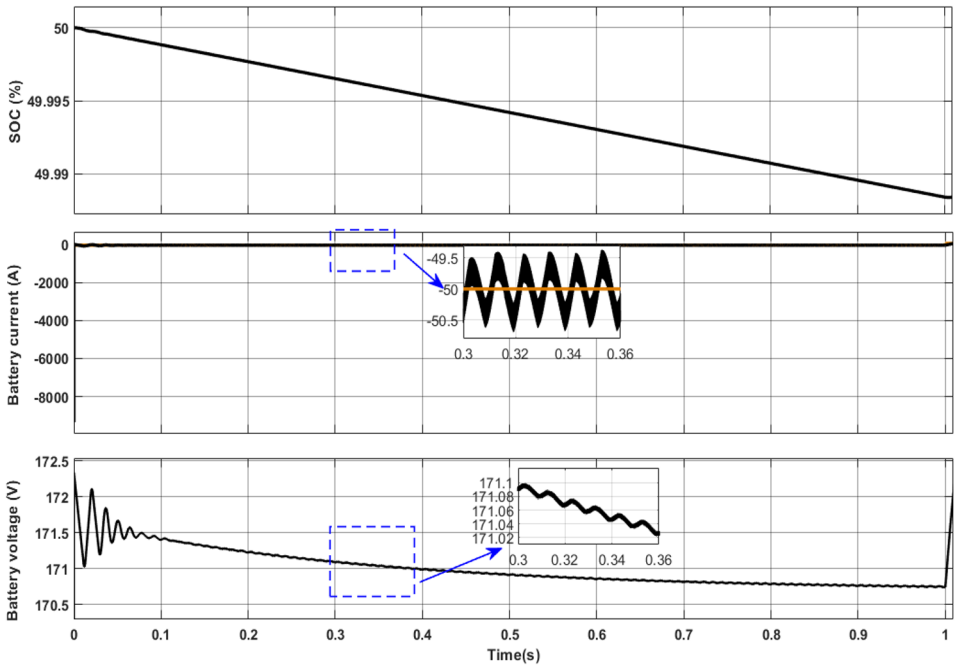

Fig. 8. EV battery SoC, current, and voltage during discharging mode (V2G)

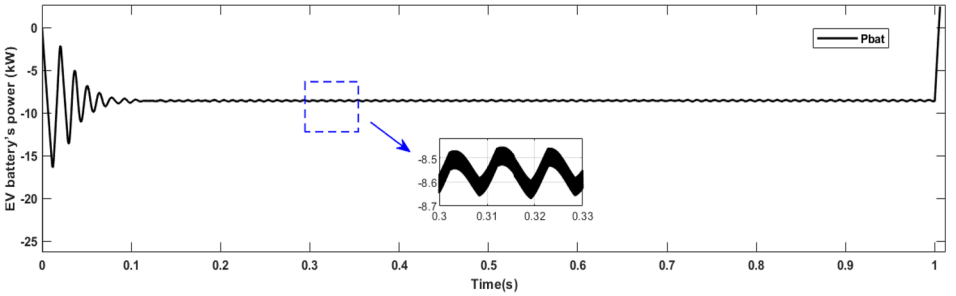

Fig. 9. EV battery's power during discharging mode (V2G)

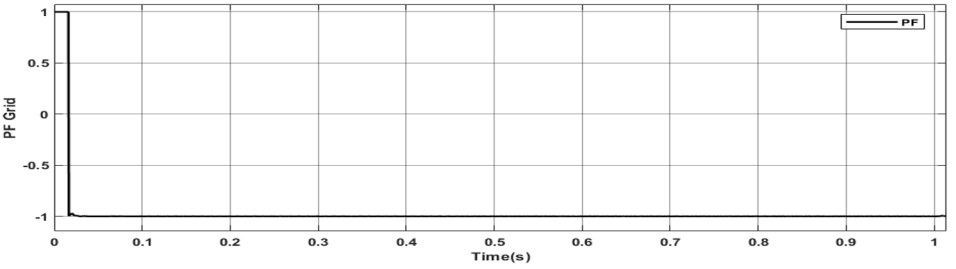

Fig. 10. PF performance during discharging mode (V2G)

4.2 Charging operation (G2V Mode)

The charging mode takes place from the grid to the EV battery, Fig. 11 shows that the input grid current is in phase with the input grid voltage Vg.

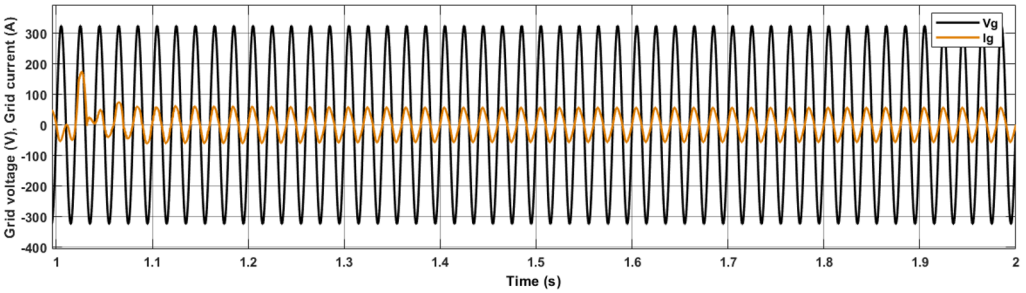

Fig. 11. Grid voltage and current during charging mode (G2V)

The efficiency derived from the simulation is demonstrated by considering the input and output power of PFC rectifier, which aligns with the calculated parameters. Moreover, as a product of the rectification process, a DC link voltage is generated for the battery side of the bidirectional DC-DC converter. The achieved DC link voltage also falls within the anticipated range, as illustrated in Fig. 12.

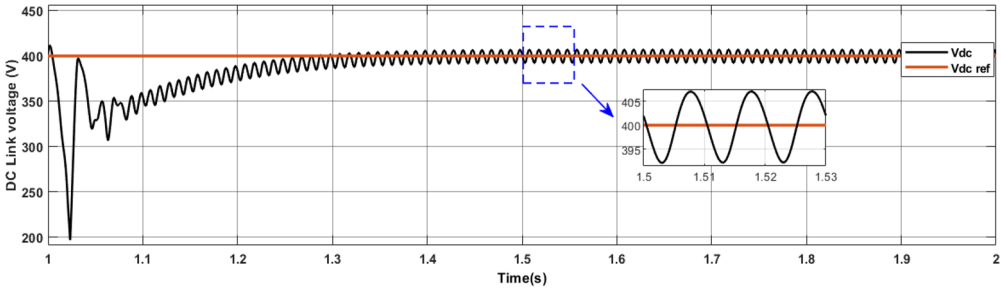

Fig. 12. DC link voltage during charging mode (G2V)

In addition, the EV battery performance is presented through the battery state of charge (SoC), charging current, and voltage, as exhibited in Fig. 13. Within the charging mode segment, the increment in SoC and the positive current value indicate the battery charging process. Correspondingly, Fig. 14 visualizes the instantaneous energy or power stored in the EV batteries. Notably, positive power values indicate the battery charging process.

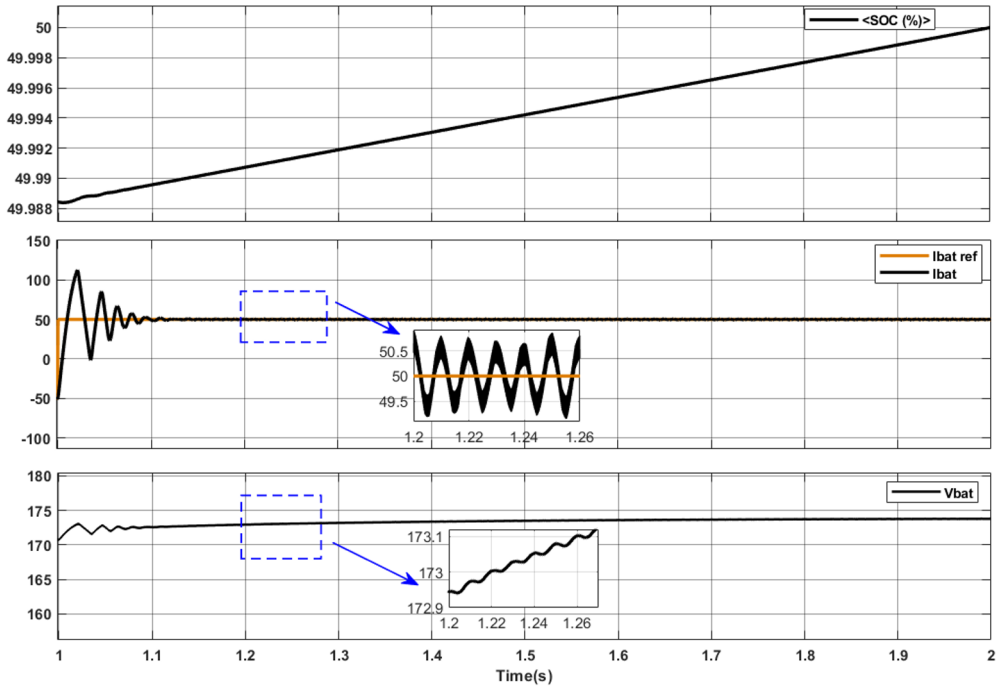

Fig. 13. EV battery SoC, current, and voltage during charging mode (G2V)

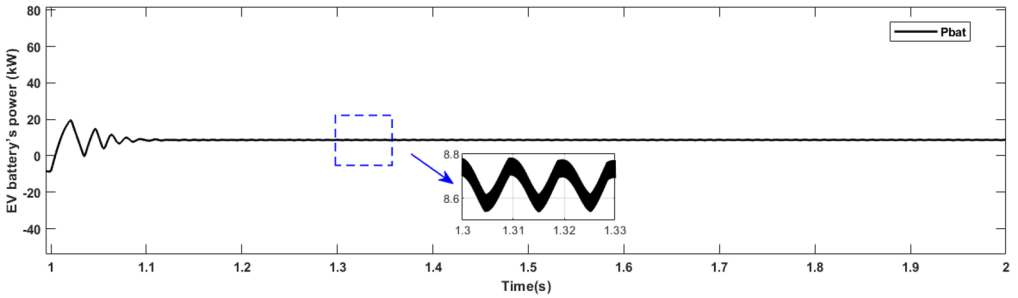

Fig. 14. EV battery power during charging mode (G2V)

Figure 15 shows that the power factor is near to unity, or in other terms, the obtained reactive power is approximately zero

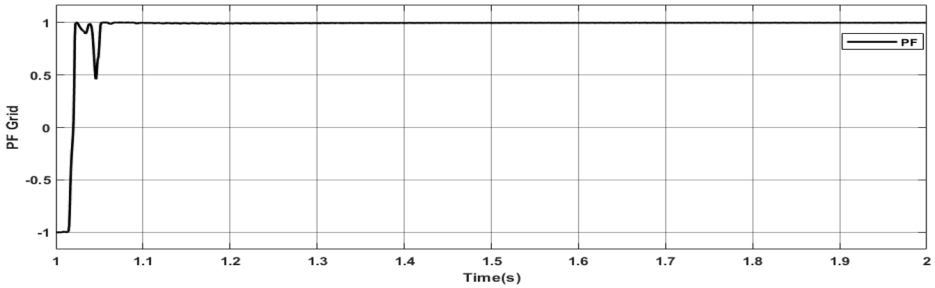

Fig. 15. PF performance during charging mode (G2V)

During the simulation of the proposed converter, two notable challenges were encountered. Firstly, achieving precise voltage regulation and control stability under varying load conditions and battery states proved to be a complex task. This was addressed by implementing a sophisticated control algorithm, and well passive components design. Secondly, there was a notable simulation waiting time to observe results due to the complexity of the model and the need for accurate transient analysis. This challenge was mitigated by optimizing the simulation settings. These solutions ensured the accurate representation of the converter's performance in the simulation results.

5 Conclusion

In this paper, a bi-directional EV charger is presented and analysed in order to enhance the EV charging process and inject power back to the grid. However, during a charging process or grid-to-vehicle operating mode, the system incorporates the bi-directional AC-DC and the bi-directional DC-DC converters that function as a rectifier and buck converter, respectively. Conversely, in the discharging process or vehicle-to-grid operating mode, these converters would be operated as an inverter and boost converter, respectively.

Furthermore, a 2kW prototype have been validated within MATLAB/Simulink environment. The system dynamic performances underscore the efficacy of the employed control strategies in both grid-to-vehicle and vehicle-to-grid modes, aligning with the chosen parameters and system specifications. The simulation results yield satisfactory outcomes, affirming the feasibility of bidirectional energy transfer with the developed model. Additionally, the system performance demonstrates the achievement of the targeted power factor, adhering to IEEE standards.

While the results of the simulations are promising, it's important to acknowledge certain limitations. The prototype was tested in a controlled, simulated environment. Real-world factors like varying grid conditions and non-standard loads may add complexity in actual use.

Future work will involve studying and testing a new model for a bidirectional Electric Vehicle (EV) charger. This model will probably combine a bidirectional AC-DC converter (either 2 level PFC or 3 Level NPC Inverter) with a bidirectional DC-DC converter (dual active bridge (DAB)), Moreover, a refined control system or diagram will be implemented. This research aims to improve the efficiency and integration of electric vehicles with the grid.

References

1. A. Verma and B. Singh, “An Implementation of Renewable Energy Based Grid Interactive Charging Station,” 2019 IEEE Transportation Electrification Conference and Expo (ITEC), Jun. 2019, doi: 10.1109/itec.2019.8790455.
2. A. Hassoune, M. Khafallah, A. Mesbahi, and T. Bouragba, “Power Management Strategies of Electric Vehicle Charging Station Based Grid Tied PV-Battery System,” International Journal of Renewable Energy Research (IJRER), vol. 8, no. 2, pp. 851-860, Jun. 2018.
3. S. Chakraborty, M. G. Simões, and W. E. Kramer, Eds., “Power Electronics for Renewable and Distributed Energy Systems,” Green Energy and Technology, 2013, doi: 10.1007/978-1-4471-5104-3.
4. K. Sayed and H. Gabbar, “Electric Vehicle to Power Grid Integration Using Three-Phase Three-Level AC/DC Converter and PI-Fuzzy Controller,” Energies, vol. 9, no. 7, p. 532, Jul. 2016, doi: 10.3390/en9070532.
5. S. Habib, M. M. Khan, F. Abbas, and H. Tang, “Assessment of electric vehicles concerning impacts, charging infrastructure with unidirectional and bidirectional chargers, and power flow comparisons,” International Journal of Energy Research, vol. 42, no. 11, pp. 3416–3441, Apr. 2018, doi: 10.1002/er.4033.
6. M. Moradpour and G. Gatto, “Controller Design of a New Universal Two-Phase SiC-GaN-Based DC-DC Converter for Plug-in Electric Vehicles,” 2018 IEEE 18th International Power Electronics and Motion Control Conference (PEMC), Aug. 2018, doi: 10.1109/epepemc.2018.8521884.
7. A. Sharma and S. Sharma, “Review of power electronics in vehicle-to-grid systems,” Journal of Energy Storage, vol. 21, pp. 337–361, Feb. 2019, doi: 10.1016/j.est.2018.11.022.
8. T. Peng et al., “A Single-Phase Bidirectional AC/DC Converter for V2G Applications,” Energies, vol. 10, no. 7, p. 881, Jun. 2017, doi: 10.3390/en10070881.
9. A. Hassoune, M. Khafallah, A. Mesbahi, and T. Bouragba, “Improved Control Strategies of Electric Vehicles Charging Station based on Grid Tied PV/Battery System,” International Journal of Advanced Computer Science and Applications, vol. 11, no. 3, 2020, doi: 10.14569/ijacsa.2020.0110314.

10. M. Restrepo, J. Morris, M. Kazerani, and C. A. Canizares, "Modeling and Testing of a Bidirectional Smart Charger for Distribution System EV Integration," IEEE Transactions on Smart Grid, vol. 9, no. 1, pp. 152–162, Jan. 2018, doi: 10.1109/tsg.2016.2547178.
11. R. B. Selvakumar, C. Vivekanandan, and S. Kavitha, "Two-quadrant current reversible non-isolated DC-DC converter for plug-in electric vehicle chargers," AIP Conference Proceedings, 2020, doi: 10.1063/5.0000301.
12. M. C. Kisacikoglu, M. Kesler, and L. M. Tolbert, "Single-Phase On-Board Bidirectional PEV Charger for V2G Reactive Power Operation," IEEE Transactions on Smart Grid, vol. 6, no. 2, pp. 767–775, Mar. 2015, doi: 10.1109/tsg.2014.2360685.
13. J. Jo, Z. Liu, and H. Cha, "A New Design Method of LCL Filter for Single Phase Grid Connected Power Converter," 2019 International Symposium on Electrical and Electronics Engineering (ISEE), Oct. 2019, doi: 10.1109/isee2.2019.8921036.
14. I. Villanueva, N. Vázquez, J. Vaquero, C. Hernández, H. López, and R. Osorio, "L vs. LCL Filter for Photovoltaic Grid-Connected Inverter: A Reliability Study," International Journal of Photoenergy, vol. 2020, pp. 1–10, Jan. 2020, doi: 10.1155/2020/7872916.
15. I. Batarseh and H. Wei, "Power Factor Correction Circuits," Power Electronics Handbook, pp. 523–547, 2011, doi: 10.1016/b978-0-12-382036-5.00019-7.
16. S. SINGIRIKONDA et al., "Adaptive Control-Based Isolated Bi-Directional Converter for G2v& V2g Charging with Integration of the Renewable Energy Source," SSRN Electronic Journal, 2022, doi: 10.2139/ssrn.4063622.
17. R. B. Selvakumar, C. Vivekanandan, and S. Kavitha, "Two-quadrant current reversible non-isolated DC-DC converter for plug-in electric vehicle chargers," AIP Conference Proceedings, 2020, doi: 10.1063/5.0000301.
18. A. Timbus, M. Liserre, R. Teodorescu, P. Rodriguez, and F. Blaabjerg, "Evaluation of Current Controllers for Distributed Power Generation Systems," IEEE Transactions on Power Electronics, vol. 24, no. 3, pp. 654–664, Mar. 2009, doi: 10.1109/tpel.2009.2012527.
19. B. Xiao, B. Xiao, and L. Liu, "State of Health Estimation for Lithium-Ion Batteries Based on the Constant Current–Constant Voltage Charging Curve," Electronics, vol. 9, no. 8, p. 1279, Aug. 2020, doi: 10.3390/electronics9081279.
20. B.-R. Ke, Y.-H. Lin, H.-Z. Chen, and S.-C. Fang, "Battery charging and discharging scheduling with demand response for an electric bus public transportation system," Sustainable Energy Technologies and Assessments, vol. 40, p. 100741, Aug. 2020, doi: 10.1016/j.seta.2020.100741.
21. S. Rastgoo, Z. Mahdavi, M. Azimi Nasab, M. Zand, and S. Padmanaban, "Using an Intelligent Control Method for Electric Vehicle Charging in Microgrids," World Electric Vehicle Journal, vol. 13, no. 12, p. 222, Nov. 2022, doi: 10.3390/wevj13120222.